



Comparison of Cerebral Blood Flow in Regions Relevant to Cognition After Enzalutamide, Darolutamide, and Placebo in Healthy Volunteers: A Randomized Crossover Trial

Steven C. R. Williams¹ · Ndaba Mazibuko¹ · Owen O'Daly¹ · Christian Zurth² · Fiona Patrick^{1,5} · Christian Kappeler³ · Iris Kuss³ · Patricia E. Cole⁴

Accepted: 17 March 2023 / Published online: 27 April 2023
© The Author(s) 2023

Abstract

Background Off-target central nervous system (CNS) effects are associated with androgen receptor (AR)-targeting treatments for prostate cancer. Darolutamide is a structurally distinct AR inhibitor with low blood–brain barrier penetration.

Objective We compared cerebral blood flow (CBF) in grey matter and specific regions related to cognition after darolutamide, enzalutamide, or placebo administration, using arterial spin-label magnetic resonance imaging (ASL-MRI).

Methods This phase I, randomized, placebo-controlled, three-period crossover study administered single doses of darolutamide, enzalutamide, or placebo to 23 healthy males (aged 18–45 years) at 6-week intervals. ASL-MRI mapped CBF 4 h post-treatment. Treatments were compared using paired *t*-tests.

Results Drug concentrations during scans confirmed similar unbound exposure of darolutamide and enzalutamide, with complete washout between treatments. A significant localized 5.2% ($p = 0.01$) and 5.9% ($p < 0.001$) CBF reduction in the temporo-occipital cortices was observed for enzalutamide versus placebo and versus darolutamide, respectively, with no significant differences for darolutamide versus placebo. Enzalutamide reduced CBF in all prespecified regions, with significant reductions versus placebo (3.9%, $p = 0.045$) and versus darolutamide (4.4%, $p = 0.037$) in the left and right dorsolateral prefrontal cortices, respectively. Darolutamide showed minimal changes in CBF versus placebo in cognition-relevant regions.

Conclusions Darolutamide did not significantly alter CBF, consistent with its low blood–brain barrier penetration and low risk of CNS-related adverse events. A significant reduction in CBF was observed with enzalutamide. These results may be relevant to cognitive function with early and extended use of second-generation AR inhibitors, and warrant further investigation in patients with prostate cancer.

Trial Registration Number NCT03704519; date of registration: October 2018.

Plain Language Summary

Androgens, or male sex hormones, bind to androgen receptors within prostate cells and can cause growth of prostate cancer. The treatment of prostate cancer often includes drugs that bind to androgen receptors, called androgen receptor inhibitors, keeping androgens from binding to the receptors and preventing prostate cancer growth. In clinical studies, these drugs may have adverse effects on the central nervous system, or brain, including dizziness, falls, and impaired thinking and problem solving. This study compared the effects of two androgen receptor inhibitors, darolutamide and enzalutamide, and placebo

✉ Steven C. R. Williams
steve.williams@kcl.ac.uk

¹ Centre for Neuroimaging Sciences, Institute of Psychiatry, Psychology and Neuroscience, King's College London, Denmark Hill, London SE5 8AF, UK

² Clinical Pharmacology Oncology, Bayer AG, Berlin, Germany

³ Clinical Development, Oncology, Bayer AG, Berlin, Germany

⁴ Imaging Strategy Oncology, Bayer HealthCare Pharmaceuticals, Inc., Whippany, NJ, USA

⁵ Present Address: Oxford Institute of Clinical Psychology Training and Research, The Oxford Centre for Psychological Health, Oxford Health NHS Foundation Trust and University of Oxford, Oxford, UK

on blood flow in the brain. Blood flow was measured by a type of magnetic resonance imaging in healthy men after receiving a single dose of treatment. Blood flow in the brain was reduced by enzalutamide compared with both placebo and darolutamide. Darolutamide did not decrease brain blood flow. This lack of effect on brain blood flow is in line with preclinical studies that showed darolutamide's limited ability to cross the blood–brain barrier, which is the naturally occurring barrier that protects the brain from harmful substances. In clinical studies of patients with prostate cancer treated with darolutamide, adverse effects on the brain have occurred in similar proportions of patients receiving darolutamide and placebo. In contrast, enzalutamide treatment has an increased risk of adverse effects on the brain versus placebo. The results of this study provide information on the effects of these androgen receptor inhibitors on brain blood flow that may be related to their adverse effects on the brain and its functioning.

Key Points

This study evaluated the effect of darolutamide and enzalutamide on cerebral blood flow measured by arterial spin-labeled magnetic resonance imaging as a surrogate measure of the drugs' brain penetration.

Consistent with low blood–brain barrier penetration, darolutamide showed no significant reduction in cerebral blood flow compared with placebo.

In contrast, enzalutamide significantly reduced localized cerebral blood flow in all prespecified regions.

1 Introduction

Androgen deprivation therapy (ADT) is the backbone of systemic therapy for prostate cancer; however, a range of cognitive and other central nervous system (CNS) changes have been associated with ADT [1, 2]. In clinical studies, CNS-related adverse events (AEs) such as seizures, dizziness, fatigue, falls, and impaired cognitive function have been reported with ADT as well as novel androgen receptor (AR) pathway-directed therapies [1, 3]. AR expression has been reported in neural areas, such as the prefrontal cortex and the mesocorticolimbic system, which are responsible for executive function [4, 5]. Cognitive impairments can lead to functional problems related to comprehension, concentration, and memory [6]. Thus, it is important that the impact of these AR-directed therapies on CNS-related AEs be identified and managed to ensure that patient safety and quality of life are maintained [1].

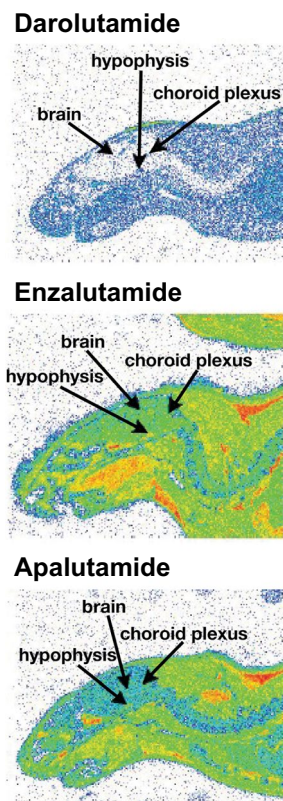
CNS-related AEs reported with AR inhibitors are thought to be associated with the penetration of the blood–brain barrier (BBB) by these drugs [7–10]. The AR inhibitors enzalutamide and apalutamide penetrate the BBB with a brain:plasma ratio of 27% and 62%, respectively, in mice [7,

8]. In the phase III PROSPER trial of patients with nonmetastatic castration-resistant prostate cancer (nmCRPC), enzalutamide was associated with an increased risk of fatigue, falls, dizziness, headache, mental impairment disorders, and seizures compared with placebo [11]. A meta-analysis found a significantly higher risk of anxiety, insomnia, headache, and restless leg syndrome in patients with metastatic CRPC receiving enzalutamide versus those receiving placebo [12]. In the phase III SPARTAN trial of patients with nmCRPC, fatigue, falls, and mental impairment disorders were reported more frequently in patients receiving apalutamide plus ADT compared with placebo plus ADT, and seizures were reported in two patients treated with apalutamide [13].

Darolutamide is a highly potent oral AR inhibitor that is structurally distinct from enzalutamide and apalutamide [8]. Preclinical pharmacokinetic studies in male mice reported a very low BBB penetration of darolutamide with a brain:plasma ratio of 1.9–3.9% following oral doses of 25, 50, or 100 mg/kg twice daily for 7 days, which was markedly lower than that observed with enzalutamide and apalutamide [8]. In an autoradiography study in male rats, *in vivo* tissue distribution after a single dose each of 10 mg/kg ¹⁴C-labeled darolutamide, enzalutamide, or apalutamide revealed a tenfold lower brain:blood ratio of ¹⁴C-labeled darolutamide compared with the other two AR inhibitors (Fig. 1) [8, 14–16]. In the phase III ARAMIS trial of patients with nmCRPC, the incidence of AEs was similar for darolutamide plus ADT and placebo plus ADT, including the CNS-related AEs of dizziness, impaired memory, cognitive disorders, and change in mental status [17, 18]. Fatigue was the only AE with an incidence > 10% in the darolutamide arm (13.2% vs. placebo, 8.3%). The incidence of AEs with darolutamide was generally lower than that reported with enzalutamide and apalutamide in the PROSPER and SPARTAN trials [11, 13, 18].

The risk of drug-associated, CNS-related AEs is likely to be determined by the drug concentration in the brain after oral administration. This study investigated changes in cerebral blood flow (CBF) using arterial spin-labeled (ASL) magnetic resonance imaging (MRI) as a proxy for brain penetration of darolutamide, enzalutamide, and placebo. The ASL-MRI technique is a reliable and consistent measure

Fig. 1 Brain distribution of [^{14}C]darolutamide, [^{14}C]enzalutamide, and [^{14}C]apalutamide at 8 h postdosing in male Wistar rats based on whole-body autoradiography [14]



	Darolutamide 10 mg/kg 8 hours [$\mu\text{g-eq/g}$]	Brain-to-Blood Ratio
Blood heart	0.870	-
Brain	0.0688	0.079
Hypothalamus	0.0527	0.061

	Enzalutamide 10 mg/kg 8 hours [$\mu\text{g-eq/g}$]	Brain-to-Blood Ratio
Blood heart	4.03	-
Brain	3.25	0.807
Hypothalamus	3.44	0.854

	Apalutamide 10 mg/kg 8 hours [$\mu\text{g-eq/g}$]	Brain-to-Blood Ratio
Blood heart	2.15	-
Brain	1.82	0.847
Hypothalamus	1.80	0.837

of resting-state CBF that can be used to assess change in CBF related to brain function following administration of a single-dose drug [19–22]. This technique has been applied to evaluation of CBF changes in individuals with mild cognitive impairment in response to memory-encoding tasks as a potential biomarker in Alzheimer disease [23].

2 Materials and Methods

2.1 Study Design

This phase I, randomized, placebo-controlled, three-period crossover study (NCT03704519) consisted of a screening visit, three treatment periods, and a follow-up visit for all participants (Fig. 2). The screening visit occurred within 35 days prior to the first treatment period and included screening MRI to assess for the presence of any structural variants or pathologic abnormalities. Each treatment period included a 1-day visit and a 42-day washout period, followed by a visit within 7 days from the end of the washout period after the third period. After completing the screening, participants were randomly assigned, using a computer-generated randomization list, to one of six different treatment sequences in which a single oral dose of darolutamide 300 mg (four tablets), enzalutamide 160 mg (four capsules), or placebo (four tablets) was administered approximately

30 min after a standardized meal on day 1. A lower dose of darolutamide than the approved treatment dose (600 mg) was used to achieve unbound plasma concentrations comparable with enzalutamide.

The study was conducted at a single study center in the UK (Center for Neuroimaging Sciences, Institute of Psychiatry, Psychology, and Neuroscience at King's College Hospital, London). The protocol was reviewed and approved by the South Central—Berkshire Research Ethics Committee and the Medical and Healthcare Regulatory Authority before study initiation. The study was conducted in accordance with the ethical principles of the Declaration of Helsinki and the International Council for Harmonisation guidelines for Good Clinical Practice, and met all local legal and regulatory requirements. All participants provided written informed consent.

2.2 Study Population

Participants were healthy males aged 18–45 years with a body mass index within the range of 18.0–30.0 kg/m². Participants were excluded if they had known contraindication to MRI, structural variants or pathologic abnormalities on screening period brain MRI, history of neurological or psychiatric disorders, ongoing medical condition involving the vital organs, diagnosed malignancy within 5 years, or had

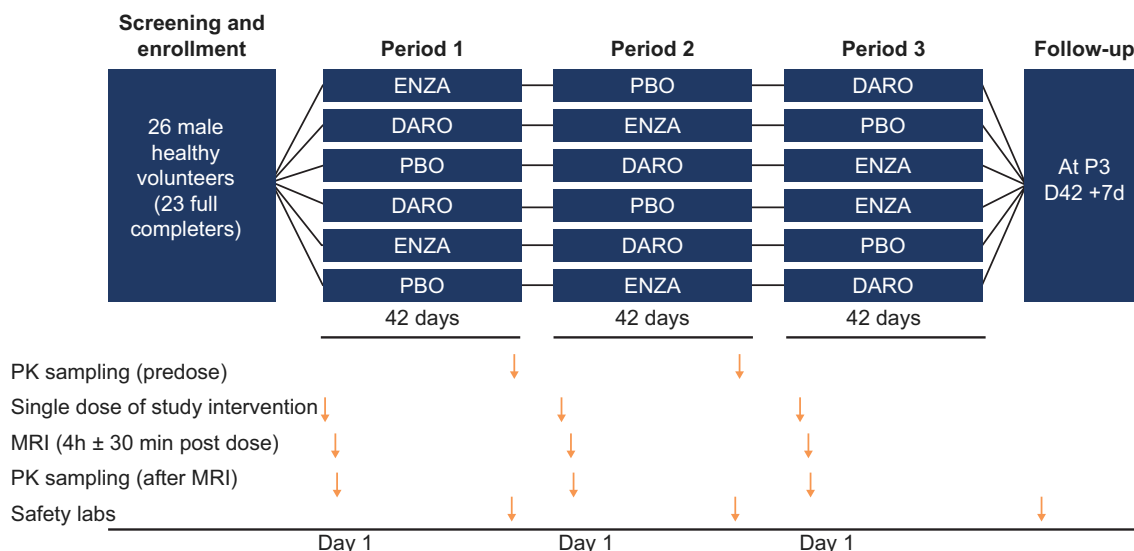


Fig. 2 Study design. Single doses of darolutamide 300 mg and enzalutamide 160 mg were administered. *D/d* day, *DARO* darolutamide, *ENZA* enzalutamide, *MRI* magnetic resonance imaging, *P3* period 3, *PBO* placebo, *PK* pharmacokinetic

received any medication that may influence the study objectives within 2 weeks prior to the start of the study.

2.3 Study Procedures

ASL-MRI scans were performed on a GE Healthcare Discovery™ MR750 3 Tesla (T) scanner using a NOVA 32-channel head coil at 4 h (± 30 min) postdose in the afternoon on day 1 of each period. At each scanning visit, a three-plane localizer and a sagittal three-dimensional (3D) T1-weighted structural sequence covering the entire brain and skull were performed. Two ASL scans (about 6 min each) were acquired in the axial plane using a pseudocontinuous arterial spin-labeling sequence (pCASL) with a multishot, segmented 3D stack of axial spirals (eight arms) readout with a resultant spatial resolution of approximately $2 \times 2 \times 3$ mm. The two ASL scans were averaged to increase signal-to-noise ratio. Labeling time was 1800 ms (a train of Hanning-shaped radiofrequency pulses) with an unbalanced labeling scheme. The post-labeling delay was 2025 ms and four inversion pulses were collected during the post-label delay. Images were obtained in an interleaved fashion, with fast spin echo (echo time of 11.1 ms), producing 512 readout points per interleave, with eight interleaves in total and four control-label pairs.

Prior to analysis, all CBF images for each participant/session were preprocessed using the standard unified segmentation-based pipeline in the Automatic Software for ASL Processing (ASAP) toolbox based on the statistical parametric mapping software (SPM version 12) run in Matlab 17b [24–26]. The images were co-registered to the high-resolution T1-weighted structural image and then

normalized to Montreal Neurological Institute (MNI) space via unified segmentation. In this process, the images were also upsampled to a resolution of $2 \times 2 \times 2$ mm. Finally, the images were smoothed by an 8-mm smoothing kernel. One proton density image was collected at the end of the series for CBF quantification, which was performed in a blinded fashion following the current ASL consensus article [27]. To minimize bias due to variation in CBF in relation to the circadian rhythm effect, dosing of study drug occurred in the morning to allow the MRI scan to be consistently performed in the afternoon for each individual.

Blood samples were collected within approximately 15 min following the completion of the MRI scan in periods 1, 2, and 3 and on day 1 prior to study drug administration for periods 2 and 3. Plasma concentrations were measured for the individual diastereomers of darolutamide and enzalutamide as well as their major metabolites keto-darolutamide and *N*-desmethyl enzalutamide.

2.4 Outcome Measures

The primary endpoints were the whole-brain analyses of voxel-by-voxel changes in global grey matter CBF derived from ASL-MRI at 4 h (± 30 min) post-treatment for the comparisons of enzalutamide versus placebo, darolutamide versus placebo, and enzalutamide versus darolutamide. Secondary endpoints were changes in mean CBF in prespecified regions of interest (ROIs) relevant to cognitive function (i.e., the hippocampus, frontal cortex, and amygdala) as measured by ASL-MRI at 4 h (± 30 min) post-treatment for the same comparisons as the primary endpoint.

Safety was assessed by physical examination, reporting of AEs, vital signs, 12-lead electrocardiogram, and blood and urine assessments prior to each dose of study drug.

2.5 Statistical Methods

Statistical sample size estimation was not performed for this study. A published estimate of the power needed to detect a modest 10% change in perfusion in a placebo-controlled crossover design (i.e., size of change we observed in the striatum following haloperidol administration) showed that 12–18 participants would be sufficient to detect a significant change between visits [28]. The chosen sample size of 24 participants was planned to be equally assigned to the six treatment sequences. For primary endpoint analyses, paired *t* tests were performed to evaluate differences within each participant in each voxel of the whole-brain CBF maps (i.e., global grey matter) for the comparisons of enzalutamide versus placebo, darolutamide versus placebo, and enzalutamide versus darolutamide. This approach removes the influence of interparticipant variability. Results were only considered significant if they survived whole-brain family-wise error correction (<0.05) based on the cluster size. Clusters were defined using an uncorrected cluster-forming threshold of $p < 0.005$. All analyses controlled for the potential confounding effects of drug-related changes in physiologic parameters (e.g., heart rate, systolic and diastolic blood pressure).

For secondary endpoint analyses, predefined ROI analyses were carried out using regions relevant to cognition, and mean CBF values were extracted using the MarsBar ROI toolbox in SPM12 [25, 29]. ROIs were constructed a priori using the neuroimaging meta-analysis repository, NeuroSynth. Linear mixed-effects models based on Matlab 2017b [26] were used with physiology as a nuisance covariate to

compare the mean CBF in each region following study drug administration. These data underwent the same analysis as described above, and the results were considered significant with a critical alpha of 0.05 ($p < 0.05$).

The potential effects of treatment sequence were analyzed using an analysis of variance (ANOVA) including sequence, period, and treatment as fixed effects and subject (sequence) as a random effect. Point estimates (least squares means) and exploratory 90% confidence intervals (CIs) were calculated for the three comparisons in each ROI. A sequence effect was detected if the hypothesis of no sequence effect was rejected by the *F* test at an alpha significance level of 0.05.

3 Results

3.1 Participants

From October 2018 to October 2019, 26 healthy male subjects were randomized to receive study drug, and 23 subjects completed all three treatment periods and were included in the analysis (Fig. 3). Subjects had a median age of 25 years (range 19–44) and a median body mass index of 23.6 kg/m² (range 18.4–30.4).

3.2 Pharmacokinetic Evaluation

Mean plasma concentrations of study drugs and metabolites were in the expected range, with geometric means of 941 ng/mL for darolutamide and 2679 ng/mL for enzalutamide at approximately 4 h postdosing (Table 1). Unbound drug concentration is considered more relevant for the ability to penetrate the BBB and was calculated for both compounds with correction for differences in their pharmacokinetic

Fig. 3 Participant disposition. Protocol deviation: subject did not meet study entry criteria because he was participating in another clinical trial at the same time. AE: Subject had cough of moderate intensity 2 days after receiving placebo and withdrew from further dosing. Other: subject emigrated and was no longer able to attend study visits. A enzalutamide—placebo—darolutamide, AE adverse event, B darolutamide—enzalutamide—placebo, C placebo—darolutamide—enzalutamide, D darolutamide—placebo—enzalutamide, E enzalutamide—darolutamide—placebo, F placebo—enzalutamide—darolutamide

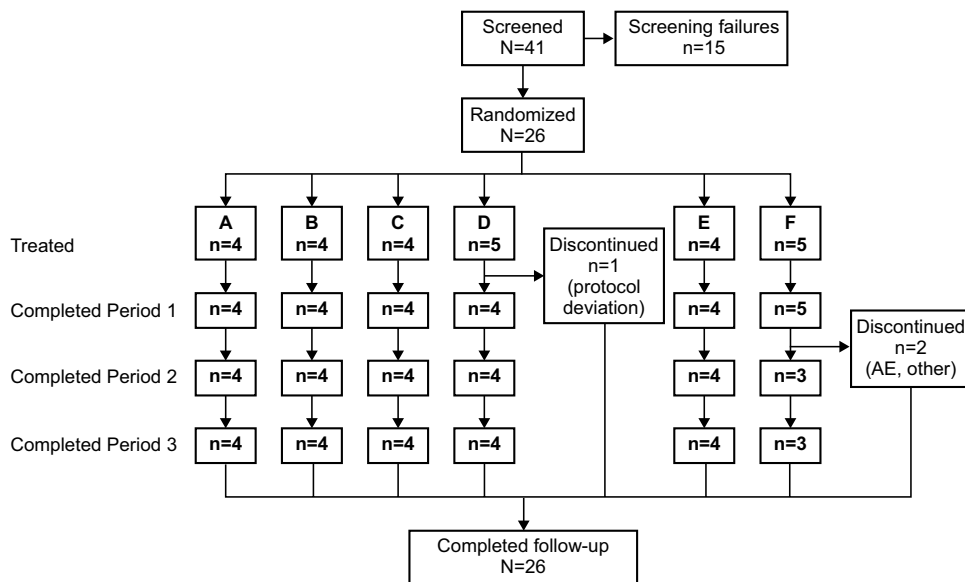


Table 1 Geometric mean (% coefficient of variation) of total pharmacokinetic concentrations of all analytes in plasma

Geometric mean (%CV) concentration at study times	Enzalutamide (ng/mL)	<i>N</i> -desmethyl enzalutamide (ng/ mL)	Darolutamide (ng/mL)	(S,R)-darolu- tamide (ng/ mL)	(S,S)-darolu- tamide (ng/ mL)	Keto-darolu- tamide (ng/mL)
Post MRI (<i>n</i> =24)	2679 (31%)	102 (60%)	941 (38%)	187 (45%)	745 (41%)	2076 (43%)
42 Days postdose [predose] ^a (<i>n</i> =16)	<LLOQ ^b	<LLOQ ^b	<LLOQ	<LLOQ	<LLOQ	<LLOQ

CV coefficient of variation, LLOQ lower limit of quantification, MRI magnetic resonance imaging

^aIn periods 2 and 3 on day 1 at predose, a pharmacokinetic sample was drawn to assess drug level at the end of the respective washout period; therefore, these values are assigned to the treatment of the previous period in this table

characteristics, including molecular weights, half-lives (darolutamide, 20 h; enzalutamide, 4 days) and protein binding (darolutamide, 92%; enzalutamide, 98%) [30, 31]. The respective unbound geometric mean concentrations were 189 nmol/L for darolutamide and 115 nmol/L for enzalutamide, which represent approximately 20% of the unbound concentration of both compounds observed at steady-state following administration of darolutamide 600 mg twice daily or enzalutamide 160 mg once daily (Fig. 4) [32]. There were no measurable predose concentrations of study drug at treatment periods 2 and 3, indicating complete washout of darolutamide and enzalutamide prior to the next study drug administration.

3.3 Primary Endpoint

Whole-brain grey matter (i.e., global grey mean) showed a 3.5% reduction in CBF for enzalutamide compared with placebo and a 3.3% reduction in CBF for enzalutamide compared with darolutamide. There was no meaningful change in grey matter CBF for darolutamide versus placebo (0.1%). Whole-brain voxel-wise analysis found evidence in the temporo-occipital cortices of statistically significant localized

reductions in CBF of 5.2% (cluster-wise pFWE_{corr} = 0.019; cluster extent of 4442 voxels) for enzalutamide compared with placebo, and 5.9% (cluster-wise pFWE_{corr} < 0.005, cluster extent of 6740 voxels) for enzalutamide versus darolutamide, but there was no significant CBF reduction for darolutamide compared with placebo (-0.7%) (Fig. 5). Comparison of enzalutamide and darolutamide identified a significant reduction in temporo-occipital CBF, which extended into the right superior, middle, and inferior temporal gyrus, the right middle and inferior occipital gyrus, the temporo-occipital area, and the right angular gyrus/temporoparietal junction.

3.4 Secondary Endpoints

Analysis of prespecified ROIs relevant to cognition showed consistent reductions in CBF with enzalutamide compared with darolutamide or placebo, but minimal changes for the comparison of darolutamide and placebo (Table 2). In the left dorsolateral prefrontal cortex, a significant reduction in CBF was observed for enzalutamide versus placebo (3.9%; *p* = 0.045) [Fig. 6]. In the right dorsolateral prefrontal cortex, a significant reduction was observed for enzalutamide versus

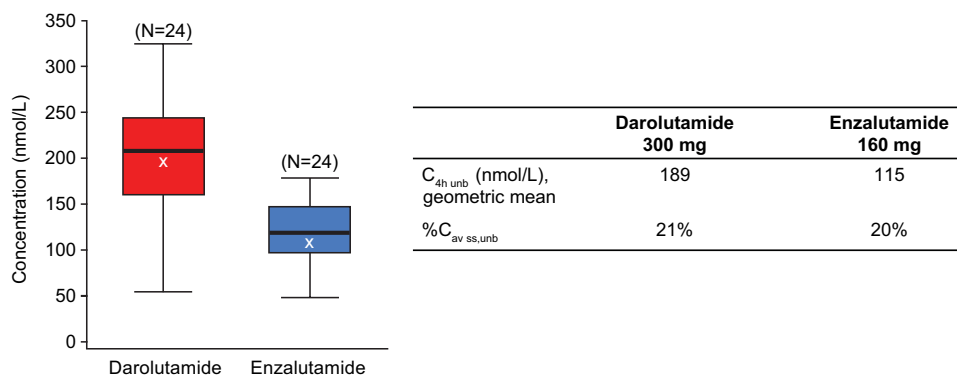


Fig. 4 Observed unbound plasma concentration of darolutamide and enzalutamide post-MRI ($C_{4h\ unbound}$). Single doses of darolutamide 300 mg and enzalutamide 160 mg were administered. Box: 25th to 75th percentile; horizontal line: median; χ : geometric mean; vertical lines extend from the box to a distance of at most 1.5 interquar-

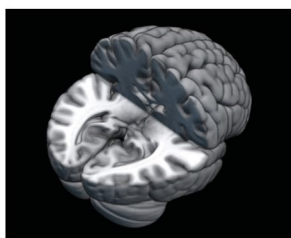
tile ranges and any value more extreme is plotted separately. $C_{4h\ unbound}$ unbound plasma concentration at 4 h postdose, $\%C_{av\ ss, unbound}$ unbound plasma concentration as a percentage of average steady-state concentration, MRI magnetic resonance imaging

Fig. 5 Localized change in whole-brain grey matter cerebral blood flow in the temporo-occipital cortices. Data presented are mean \pm standard error of the mean. Colored areas in three-dimensional brain figures indicate regions of significant difference in regional CBF between a pair of study interventions. These images are family-wise error-corrected statistical maps derived from all participants overlaid on an anatomic image. A cluster-forming threshold of $p < 0.005$ uncorrected was used. All measures were corrected for physiologic covariates (i.e., heart rate, systolic and diastolic blood pressure). *CBF* cerebral blood flow

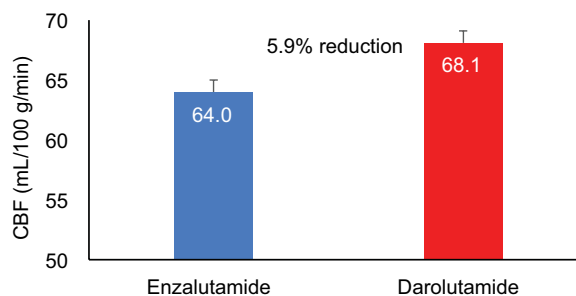
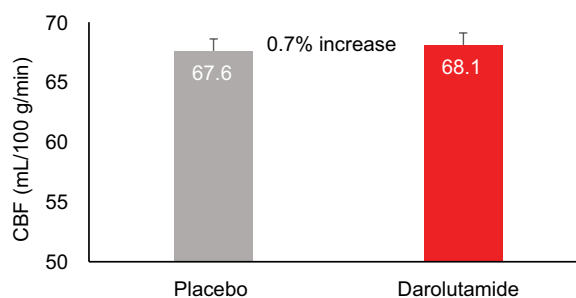
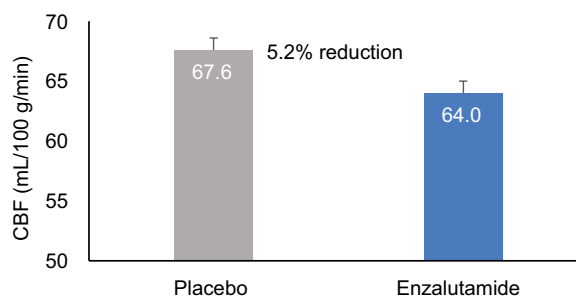
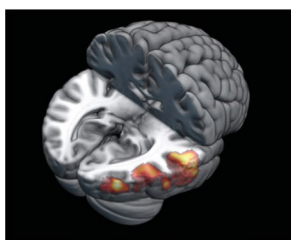
Placebo vs Enzalutamide



Placebo vs Darolutamide



Enzalutamide vs Darolutamide



darolutamide (4.4%; $p = 0.037$). Notable CBF changes that did not reach statistical significance included enzalutamide versus darolutamide in the left dorsolateral prefrontal cortex (-2.9%) and enzalutamide versus placebo in the right dorsolateral prefrontal cortex (-3.4%). Consistent reductions in localized CBF were observed for the left and right hippocampus, both anterior and whole, for enzalutamide compared with placebo and enzalutamide compared with darolutamide, but the differences did not reach statistical significance. Differences in CBF in the dorsolateral prefrontal cortex and hippocampus between darolutamide and placebo were negligible and not significant. After correction for multiple comparisons, no statistically significant differences were observed in any of the predefined ROIs, and no effects of treatment sequence were found in the ROIs.

3.5 Safety

The study drugs were well tolerated. Fifteen of 26 subjects (57.7%) experienced at least one AE of mild or moderate intensity, with 25.0%, 29.2%, and 28.0% of subjects experiencing AEs after receiving darolutamide, enzalutamide,

and placebo, respectively. Eight AEs in six subjects (23.1%) were considered study drug-related and occurred in all three treatment groups: headache for darolutamide and enzalutamide, and headache and dizziness for placebo. One subject experienced an unrelated serious AE (cerebral infarction) that occurred after he had completed study drug administration for all three periods, and one subject experienced an unrelated AE (cough), which led to discontinuation of study drug. No clinically relevant changes in safety laboratory values, vital signs, or electrocardiogram parameters were observed at any time during the study.

4 Discussion

This is the first study using CBF, as assessed by ASL-MRI, as an indirect measure of brain penetration between ARIs, darolutamide and enzalutamide, and placebo. ASL-MRI is a non-invasive technique for assessing tissue perfusion by measuring blood flow. This technique identified greater central effects on brain physiology with enzalutamide relative to placebo and darolutamide. Significantly reduced CBF was observed with

Table 2 Cerebral blood flow in the global grey matter and predefined regions of interest by treatment and differences between treatments

Region	Darolutamide	Placebo	Enzalutamide	Placebo–darolutamide	Darolutamide–enzalutamide	Placebo–enzalutamide
	mL/100 g/min	mL/100 g/min	mL/100 g/min	% Difference	% Difference	% Difference
Primary endpoints (whole-brain grey matter)						
Global grey mean ^a	55.4	55.5	53.5	−0.14	−3.32	−3.46
Temporo-occipital ^a	68.1	67.6	64.0	0.73	−5.91 ^b	−5.22 ^b
Secondary endpoints (predefined regions)						
Anterior cingulate	66.4	66.0	64.1	0.71	−3.59	−2.89
L amygdala	51.6	51.4	50.3	0.31	−2.44	−2.13
R amygdala	50.5	50.9	49.0	−0.70	−3.02	−3.70 ^c
L dorsolateral prefrontal cortex	56.0	56.5	54.3	−0.99	−2.92	−3.87 ^c
R dorsolateral prefrontal cortex	58.0	57.4	55.5	1.00	−4.39 ^c	−3.43
Dorsomedial prefrontal cortex	57.2	57.1	55.5	0.21	−2.90	−2.70
L ventrolateral prefrontal cortex	64.1	64.3	62.5	−0.31	−2.38	−2.68
R ventrolateral prefrontal cortex	61.0	60.8	59.0	0.29	−3.28	−2.99
Ventromedial prefrontal cortex	63.3	62.8	61.0	0.79	−3.58	−2.80
L anterior hippocampus	51.2	50.9	49.6	0.64	−3.12	−2.50
R anterior hippocampus	49.3	49.6	48.2	−0.73	−2.28	−2.98
L whole hippocampus	51.2	50.9	49.6	0.57	−3.04	−2.49
R whole hippocampus	48.9	49.2	47.6	−0.59	−2.57	−3.15
L parahippocampal gyrus	50.4	50.3	48.8	0.36	−3.17	−2.82
R parahippocampal gyrus	48.6	49.1	47.7	−0.97	−1.79	−2.73
L ventral striatum	57.2	57.4	55.8	−0.34	−2.46	−2.78
R ventral striatum	57.1	57.7	56.1	−0.89	−1.83	−2.70

Negative percentage difference values indicate a reduction in CBF following drug administration (i.e., placebo > drug); positive values indicate drug-related increases (i.e., drug > placebo) in CBF

CBF cerebral blood flow, FWE family-wise error, L left, R right

^aUsing voxel-based analysis of whole-brain grey matter

^bStatistically significant ($p_{FWE} < 0.05$)

^cStatistically significant ($p < 0.05$ prior to Bonferroni correction for multiple comparisons)

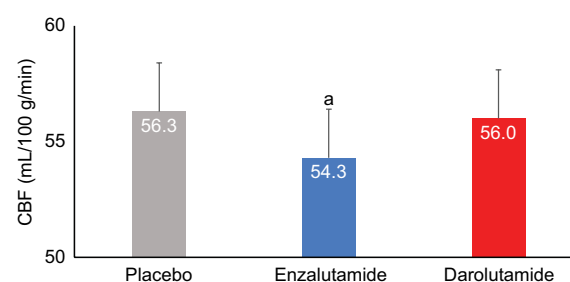


Fig. 6 Region of interest analysis of cerebral blood flow changes in the left dorsolateral prefrontal cortex. Colored area in the 3D brain figure represents the brain area, which was prespecified from an atlas. Data presented are mean \pm standard error of the mean CBF for the

colored region depicted in the 3D brain figure for each treatment condition. ^aFor enzalutamide versus placebo, $t_{(22)} = 2.06$; $p = 0.045$. 3D three-dimensional, CBF cerebral blood flow

enzalutamide compared with darolutamide or placebo, while no meaningful difference in CBF was observed between darolutamide and placebo, indicating less penetration of darolutamide into the brain. These results are consistent with prior preclinical studies that showed a tenfold lower BBB penetration of darolutamide versus enzalutamide [8, 14–16]. These data are also in line with the clinical safety profile of darolutamide, which shows similar incidence of CNS-related AEs between darolutamide and placebo in patients with nmCRPC [17, 18]. In the ARAMIS study, fatigue was reported in 13.2% of patients receiving darolutamide and 8.3% of those receiving placebo; rates of mental-impairment disorder (2.0% vs. 1.8%) and dizziness, including vertigo (4.5% vs. 4.0%), were minimally different between treatment groups [18].

CNS-related AEs are thought to be associated with the brain penetration of drugs [3, 7–10]; therefore, these data suggest that darolutamide has low potential to cause CNS-related AEs that can impact a patient's daily life. Significant reductions in CBF after enzalutamide treatment were localized, in part, to the temporo-occipital regions, which have several important cognitive and perceptual roles. For example, the superior temporal gyrus is integral to auditory processing [33], the temporoparietal junction is associated with the attentional network [34], and the angular gyrus is an integration hub, combining multisensory inputs for problem solving and attentional orientation [35]. Although causality is beyond the scope of this experiment, these functions are integral to daily life, and aberrant functioning arising from AR-directed therapy is not desirable. Several of the ROIs investigated in our study (hippocampus, amygdala) have been recently shown to have high AR-RNA expression using regional homogeneity and functional connectivity methods, highlighting increased interest in this area of study [36].

Altered CBF in the right amygdala and the dorsolateral prefrontal cortex after enzalutamide treatment is consistent with prior research, suggesting a role for androgen changes (via hypogonadism or gonadectomy) in reducing executive functioning and in the presence of mood disorders [5]. The dorsolateral prefrontal cortex is prominently involved in executive functioning, including the representation of task goals held in memory for the internal evaluation of one's performance [37, 38] and control of cognitive processes for planning and reasoning [39]. Thus, the demonstration of altered CBF within this area has the potential to reduce oxygenation and impact executive functioning. In addition, decreased blood flow in the dorsolateral prefrontal cortex has been noted in depressed individuals, suggesting a negative impact on emotional regulation [40]. This finding is supported by a previous paper that identified higher scores on the Patient Health Questionnaire-9, a measure of depression, in individuals with metastatic CRPC treated with enzalutamide versus abiraterone [41].

The three-way crossover design of this study allowed intrasubject comparison of the effects of darolutamide and

enzalutamide on brain perfusion, with the placebo providing a measure of amplitude of noise relative to the study drugs. The use of six treatment sequence groups avoided the potential bias of a fixed dosing sequence. However, the study was limited by a population that consisted of subjects who were younger than those who are traditionally affected with prostate cancer. An older population would be of interest as increasing age has been linked to greater BBB permeability [42]. The advantage of investigating all three treatments in a crossover design resulted in the limitation of single-dose administration for all treatments. With single-dose administration, the full exposure of enzalutamide and darolutamide, as observed during steady-state, could not be achieved in plasma. Administration, dose, and imaging time were selected to reach similar unbound concentrations of both compounds after single-dose administration, reflecting the relationship at steady-state. The unbound plasma concentrations at the time of the MRI scan were approximately 20% of the average steady-state concentrations for both compounds. The data indicate that the observed effect on CBF changes after single-dose administration may be even more pronounced when steady-state concentrations are reached. The impact of these changes in CBF on behavior and cognitive function after continuous treatment also warrants further investigation.

5 Conclusion

Enzalutamide significantly reduced CBF compared with both placebo and darolutamide, while darolutamide was not associated with significant reductions in localized CBF compared with placebo. These results support preclinical evidence showing low BBB penetration of darolutamide. Treatment-induced reduction in CBF may translate into changes in brain activity in areas, such as the frontal cortex, that may be relevant to cognitive function (e.g., executive function, memory, and anxiety). Further investigation in patients with prostate cancer is warranted.

Acknowledgements The authors thank Dr. Hille Gieschen (Bayer Pharmaceuticals, Berlin, Germany) and colleagues for the images from the rat autoradiography study. Medical writing support was provided by Open Health Medical Communications (London, UK), supported by Bayer. Steven C. R. Williams wishes to thank the Wellcome Trust and the National Institute for Health Research (NIHR) Maudsley Biomedical Research Centre at South London and Maudsley NHS Foundation Trust and King's College London for their continued provision of facilities and support of our neuroimaging research.

Declarations

Funding This work was supported by Bayer HealthCare.

Conflict of Interest Steven C. R. Williams and Ndaba Mazibuko report research funding from Bayer, provided to the institution. Christian

Zurth, Christian Kappeler, Iris Kuss, and Patricia E. Cole are employees of Bayer. Owen O'Daly and Fiona Patrick have no disclosures to declare.

Ethics Approval This study was conducted at a single study center in the UK (Center for Neuroimaging Sciences, Institute of Psychiatry, Psychology, and Neuroscience at King's College Hospital, London). The protocol was reviewed and approved by the South Central—Berkshire Research Ethics Committee and the Medical and Healthcare Regulatory Authority before study initiation. The study was conducted in accordance with the ethical principles of the Declaration of Helsinki and the International Council for Harmonisation guidelines for Good Clinical Practice, and met all local legal and regulatory requirements. All participants provided written informed consent.

Consent to Participate Written informed consent was obtained from all individual participants in the study.

Consent for Publication All authors reviewed and approved the manuscript submitted for publication and are responsible for the correctness of the statements provided in the manuscript.

Data Availability Availability of the data underlying this publication will be determined according to Bayer's commitment to the EFPIA/PhRMA 'Principles for responsible clinical trial data sharing'. This pertains to scope, timepoint and process of data access. As such, Bayer commits to sharing, upon request from qualified scientific and medical researchers, patient-level clinical trial data, study-level clinical trial data, and protocols from clinical trials in patients for medicines and indications approved in the United States (US) and European Union (EU) as necessary for conducting legitimate research. This applies to data on new medicines and indications that have been approved by the EU and US regulatory agencies on or after 1 January 2014. Interested researchers can use <https://www.vivli.org> to request access to anonymized patient-level data and supporting documents from clinical studies to conduct further research that can help advance medical science or improve patient care. Information on the Bayer criteria for listing studies and other relevant information is provided in the member section of the portal. Data access to anonymized patient-level data, protocols and clinical study reports will be granted after approval by an independent scientific review panel. Bayer is not involved in the decisions made by the independent review panel, and will take all necessary measures to ensure that patient privacy is safeguarded.

Code Availability Not applicable.

Author Contributions Conceptualization: SCRW, IK, PEC. Methodology: SCRW, OO'D, CZ, FP, CK, PEC. Formal analysis and investigation: SCRW, NM, OO'D, CZ, FP, PEC. Writing – original draft preparation: SCRW, OO'D, FP. Writing – review and editing: SCRW, NM, OO'D, CZ, FP, CK, IK, PEC. Funding acquisition: SCRW. Resources: SCRW. Supervision: SCRW, NM. All authors participated in the critical review and revision of this manuscript and provided approval of the manuscript for submission.

Open Access This article is licensed under a Creative Commons Attribution-NonCommercial 4.0 International License, which permits any non-commercial use, sharing, adaptation, distribution and reproduction in any medium or format, as long as you give appropriate credit to the original author(s) and the source, provide a link to the Creative Commons licence, and indicate if changes were made. The images or other third party material in this article are included in the article's Creative Commons licence, unless indicated otherwise in a credit line to the material. If material is not included in the article's Creative Commons licence and your intended use is not permitted by statutory

regulation or exceeds the permitted use, you will need to obtain permission directly from the copyright holder. To view a copy of this licence, visit <http://creativecommons.org/licenses/by-nc/4.0/>.

References

1. Ryan C, Wefel JS, Morgans AK. A review of prostate cancer treatment impact on the CNS and cognitive function. *Prostate Cancer Prostatic Dis.* 2020;23:207–19.
2. Tae BS, Jeon BJ, Shin SH, Choi H, Bae JH, Park JY. Correlation of androgen deprivation therapy with cognitive dysfunction in patients with prostate cancer: a nationwide population-based study using the national health insurance service database. *Cancer Res Treat.* 2019;51:593–602.
3. Wefel JS, Ryan CJ, Van J, Jackson JC, Morgans AK. Assessment and management of cognitive function in patients with prostate cancer treated with second-generation androgen receptor pathway inhibitors. *CNS Drugs.* 2022;36:419–49.
4. Low KL, Ma C, Soma KK. Tyramide signal amplification permits immunohistochemical analyses of androgen receptors in the rat prefrontal cortex. *J Histochem Cytochem.* 2017;65:295–308.
5. Tobiansky DJ, Wallin-Miller KG, Floresco SB, Wood RI, Soma KK. Androgen regulation of the mesocorticolimbic system and executive function. *Front Endocrinol (Lausanne).* 2018;9:279.
6. Wu LM, Diefenbach MA, Gordon WA, Cantor JB, Cherrier MM. Cognitive problems in patients on androgen deprivation therapy: a qualitative pilot study. *Urol Oncol.* 2013;31:1533–8.
7. Clegg NJ, Wongvipat J, Joseph JD, et al. Arn-509: a novel antiandrogen for prostate cancer treatment. *Cancer Res.* 2012;72:1494–503.
8. Moilanen AM, Riikonen R, Oksala R, et al. Discovery of odm-201, a new-generation androgen receptor inhibitor targeting resistance mechanisms to androgen signaling-directed prostate cancer therapies. *Sci Rep.* 2015;5: 12007.
9. Shore ND, Bono P, Massard C, Snapir A, Sarapohja T, Fizazi K. Odm-201 and the CNS: a clinical perspective [abstract]. *J Clin Oncol.* 2014;32(4 Suppl):275.
10. Merriman JD, Von Ah D, Miaskowski C, Aouizerat BE. Proposed mechanisms for cancer- and treatment-related cognitive changes. *Semin Oncol Nurs.* 2013;29:260–9.
11. Hussain M, Fizazi K, Saad F, et al. Enzalutamide in men with nonmetastatic, castration-resistant prostate cancer. *N Engl J Med.* 2018;378:2465–74.
12. Sanchez Iznola M, Parra R, Angela G, Casariego J, Muñoz Del Toro J, Robinson P. Neuropsychiatric adverse events of enzalutamide and abiraterone acetate plus prednisone treatment: contrasting a meta-analysis of randomized clinical trials with real world reporting patterns from eudra [abstract 831p]. *Ann Oncol.* 2017;28(Suppl 5):289.
13. Smith MR, Saad F, Chowdhury S, et al. Apalutamide treatment and metastasis-free survival in prostate cancer. *N Engl J Med.* 2018;378:1408–18.
14. Sandmann S, Trummel D, Seidel D, Nubbemeyer R, Gieschen H, Zurth C. Higher blood–brain barrier penetration of [¹⁴C]apalutamide and [¹⁴C]enzalutamide compared to [¹⁴C]darolutamide in rats using whole-body autoradiography [poster]. Presented at the Annual Genitourinary Cancers Symposium, 14–16 February 2019, San Francisco.
15. Zurth C, Sandmann S, Trummel D, Seidel D, Gieschen H. Blood–brain barrier penetration of [¹⁴C]darolutamide compared with [¹⁴C]enzalutamide in rats using whole body autoradiography [abstract]. *J Clin Oncol.* 2018;36(6 Suppl):345.

16. Zurth C, Sandman S, Trummel D, Seidel D, Nubbemeyer R, Gieschen H. Higher blood–brain barrier penetration of [¹⁴C]apalutamide and [¹⁴C]enzalutamide compared to [¹⁴C]darolutamide in rats using whole-body autoradiography [abstract]. *J Clin Oncol*. 2019;37(7 Suppl):156.
17. Fizazi K, Shore N, Tammela TL, et al. Darolutamide in non-metastatic, castration-resistant prostate cancer. *N Engl J Med*. 2019;380:1235–46.
18. Fizazi K, Shore N, Tammela TL, et al. Nonmetastatic, castration-resistant prostate cancer and survival with darolutamide. *N Engl J Med*. 2020;383:1040–9.
19. Li Z, Vidorreta M, Katchmar N, Alsop DC, Wolf DH, Detre JA. Effects of resting state condition on reliability, trait specificity, and network connectivity of brain function measured with arterial spin labeled perfusion MRI. *Neuroimage*. 2018;173:165–75.
20. Handley R, Zelaya FO, Reinders AA, et al. Acute effects of single-dose aripiprazole and haloperidol on resting cerebral blood flow (RCBF) in the human brain. *Hum Brain Mapp*. 2013;34:272–82.
21. Marquand AF, O’Daly OG, De Simoni S, et al. Dissociable effects of methylphenidate, atomoxetine and placebo on regional cerebral blood flow in healthy volunteers at rest: a multi-class pattern recognition approach. *Neuroimage*. 2012;60:1015–24.
22. Hawkins PCT, Wood TC, Vernon AC, et al. An investigation of regional cerebral blood flow and tissue structure changes after acute administration of antipsychotics in healthy male volunteers. *Hum Brain Mapp*. 2018;39:319–31.
23. Xie L, Dolui S, Das SR, et al. A brain stress test: cerebral perfusion during memory encoding in mild cognitive impairment. *Neuroimage Clin*. 2016;11:388–97.
24. Mato Abad V, García-Polo P, O’Daly O, Hernández-Tamames JA, Zelaya F. Asap (automatic software for asl processing): a toolbox for processing arterial spin labeling images. *Magn Reson Imaging*. 2016;34:334–44.
25. SPM12 software—statistical parametric mapping. UCL Queen Square Institute of Neurology; 2020. <https://www.fil.ion.ucl.ac.uk/spm/software/spm12/>. Accessed 3 Jun 2021.
26. Matlab version 9.3. The MathWorks, Inc.; 2017. <https://www.mathworks.com/products/statistics.html>. Accessed 6 May 2021.
27. Alsop DC, Detre JA, Golay X, et al. Recommended implementation of arterial spin-labeled perfusion MRI for clinical applications: a consensus of the ISMRM perfusion study group and the European Consortium for ASL in Dementia. *Magn Reson Med*. 2015;73:102–16.
28. Murphy K, Harris AD, Diukova A, et al. Pulsed arterial spin labeling perfusion imaging at 3 T: estimating the number of subjects required in common designs of clinical trials. *Magn Reson Imaging*. 2011;29:1382–9.
29. Brett M, Anton J-L, Valabregue R, Poline J-B. Region of interest analysis using an spm toolbox [abstract 497]. Presented at the International Conference on Functional Mapping of the Human Brain, 2–6 June 2002, Sendai.
30. Nubeqa [package insert]. Whippany: Bayer HealthCare Pharmaceuticals; 2021.
31. Gibbons JA, Ouatas T, Krauwinkel W, et al. Clinical pharmacokinetic studies of enzalutamide. *Clin Pharmacokinet*. 2015;54:1043–55.
32. Gibbons JA, de Vries M, Krauwinkel W, et al. Pharmacokinetic drug interaction studies with enzalutamide. *Clin Pharmacokinet*. 2015;54:1057–69.
33. Bigler ED, Mortensen S, Neeley ES, et al. Superior temporal gyrus, language function, and autism. *Dev Neuropsychol*. 2007;31:217–38.
34. Krall SC, Rottschy C, Oberwelland E, et al. The role of the right temporoparietal junction in attention and social interaction as revealed by ale meta-analysis. *Brain Struct Funct*. 2015;220:587–604.
35. Seghier ML. The angular gyrus: multiple functions and multiple subdivisions. *Neuroscientist*. 2013;19:43–61.
36. Plata-Bello J, Plata-Bello A, Pérez-Martín Y, et al. Changes in resting-state measures of prostate cancer patients exposed to androgen deprivation therapy. *Sci Rep*. 2021;11: 23350.
37. Stuss DT. Functions of the frontal lobes: relation to executive functions. *J Int Neuropsychol Soc*. 2011;17:759–65.
38. Fassbender C, Murphy K, Foxe JJ, et al. A topography of executive functions and their interactions revealed by functional magnetic resonance imaging. *Brain Res Cogn Brain Res*. 2004;20:132–43.
39. Koechlin E, Ody C, Kouneiher F. The architecture of cognitive control in the human prefrontal cortex. *Science*. 2003;302:1181–5.
40. Bench CJ, Friston KJ, Brown RG, Scott LC, Frackowiak RS, Dolan RJ. The anatomy of melancholia—focal abnormalities of cerebral blood flow in major depression. *Psychol Med*. 1992;22:607–15.
41. Khalaf DJ, Sunderland K, Eigl BJ, et al. Health-related quality of life for abiraterone plus prednisone versus enzalutamide in patients with metastatic castration-resistant prostate cancer: results from a phase II randomized trial. *Eur Urol*. 2019;75:940–7.
42. Farrall AJ, Wardlaw JM. Blood-brain barrier: ageing and microvascular disease—systematic review and meta-analysis. *Neurobiol Aging*. 2009;30:337–52.